Back to Session Subjects

Measurement of In-Flight Rotor Blade Loads of an Autogyro

Helmut Rapp, Peter Wedemeyer
Institut für Aerospace-Technologie, Hochschule Bremen, Bremen, Germany
Christian Teuber
STN Atlas Elektronik GmbH, Bremen, Germany

Abstract

Autogyros, or gyroplanes, are rotary wing aircraft with no driven main rotor. The rotor keeps rotating only by the airflow resulting from the plane's forward speed. Since WW2 there has been only a few investigations concerning the flying characteristics and performance of autogyros including blade loading.

This work covers both the theoretical and experimental investigations of rotor blade loading. The main parameters for the flapping moment are rotor speed and mass distribution of the rotor blades. For the experimental investigations, a small telemetric system was developed. Up to four strains in the rotor blades can be measured by using strain gauges. Wireless transmission of the strain data from the rotating rotor to a computer inside the fuselage is accomplished by 433 MHz transceivers. A simple data protocol to detect and correct faulty data was implemented. In addition to the strain measurements, video sequences of the rotor blade motion are recorded by a small rotor hub mounted video camera.

1. Introduction

If someone talks about the technology of autogyros this technology seems to be well known because of the commonly-known rotary wing aircraft i.e. helicopters. Since the 50's or 60's there scarcely has been any further research in this particular kind of aircraft, especially with small gyroplanes.

The autogyro, a type of aircraft originally developed in Spain in 1920, made its first successful flight on 9th January 1923 [1]. After a short period of work in Spain, major development was moved to the United Kingdom, where the military found much interest in this particular type of aircraft. Very soon other countries obtained the rights to use the patented designs for their particular developments. At this time the major research was done in the United Kingdom by Cierva Autogiro Company of Juan de la Cierva and his team and also in the United States by the American Autogiro Company of Harold F. Pitcairn and his team. Both teams in 1937 were able to develop, build and fly prototypes of helicopters.

However, both companies were always aware that the helicopter would be the more expensive to operate solution for minor operations. This lead them to go ahead in gyroplane development until there was extensive pressure due to military requirements.

In later stages their gyroplane was able to take off vertically, to proceed the so-called "Direct Take-Off" over a 10 m obstacle and a vertical landing, if required. Several gyroplanes were obtained by the US-Military and a thorough research programme was undertaken at NACA-Laboratories compared to the small research programmes done by the British, German and French military. However, due to different design the later developed Gyrocopter does not reflect the NACA results. In some short term research this type of aircraft was covered, even as a solution for a Mars-Landing-Vehicle and Pilot-Recovery-Systems. Major design effort was put into gyroplanes for the civil market, reflected in the McCulloch J-2 and Umbaugh 18A, which is still in production as a fully certified aircraft.

In Europe, development was pushed forward, finding its success in the Fairey Rotordyne, as the probably most advanced aircarrier with 68 seats. Any further development targets were too ambitious and therefore were unsuccessful, mostly due to fact that the designers' and project leader's requirements were expecting to combine helicopter and gyroplane characteristics.

Since these short studies it is not known about any further research until during the last 6 years two United States based Companies started to develop a competitor to the helicopter. They are called "Hawk" and "CarterCopter", both developments are sponsored through indirect governmental sources.

In 1993 first steps were made to establish a gyroplane aircraft class in the United Kingdom. Due to the number of complaints these regulations didn't become effective. Meanwhile, several fatal accidents with "AirCommand" gyroplanes lead the CAA to take direct action and started a research program at Glasgow University [4] [5].

In 1993, a German programme to establish the gyroplane within the Ultralight-Aircraft class began and was pushed until end of 1999. Despite notification of the requirements through the EC there has been no German progress, but France and Italy have made several decisions and pushed their regulations.

Since no progress has been in Germany, it was decided in 1997 to start a gyroplane research programme at Hochschule Bremen, a university of ap-

presented at the 26th European Rotorcraft Forum, 26 - 29 September 2000, The Hague, Netherlands

plied sciences, supported by the director of ARROW Engines (UK), Ltd., who at this time was fully involved in the German activities. This at least gives a little bit of industrial support, and the Hochschule Bremen need not obtain, maintain and handle a gyroplane and a pilot just for the reason of research and education.

Due to European connections of ARROW Engines (UK), Ltd., these research results will find their way directly into safer designs and better performance of light gyroplanes.

In the present report, a thorough investigation, using both theory and experiment, has been carried out, especially where blade loading is concerned. The basic theory for calculating blade bending moments is shown. Telemetric equipment is developed to measure in-flight blade loadings.

2. Basic autogyro theory

Basic theory of pure autorotation is well known by helicopter specialists [2], [3]. In the following the basic equations are given. The theoretical results of these equations are to be verified later by flight measurements.

2.1 Steady autorotation

Steady autorotation means that there is no forward speed with respect to the aircraft. The airflow is strictly perpendicular through the rotor plane and the loading of the blade is independent of its angular position. According to [2], total rotor thrust T follows from integration of the local air loads along the rotor:

$$T = \frac{1}{2}\rho a b c \Omega^2 R^3 \left(\frac{\theta}{3} + \frac{\lambda}{2}\right), \tag{1}$$

where ρ denotes the air density, a the slope of the lift curve, b the number of blades, c the blade chord and R the rotor disc radius. The blade section pitch angle θ is assumed to be constant over the rotor radius. For a given 1g flight condition, thrust must be equal to the known weight of the autogyro.

To determine the unkown rotor speed Ω and inflow coefficient λ, rotor torque M_T has to be considered (C_{D0}: profile drag coefficient).

$$M_T = \frac{1}{2}\rho b c \Omega^2 R^4 \left[\frac{C_{D0}}{4} - a\lambda\left(\frac{\theta}{3} + \frac{\lambda}{2}\right)\right]. \tag{2}$$

The rotor of an autogyro is not driven so the overall torque has to be zero:

$$M_T = 0. \tag{3}$$

With this, equation (2) can be solved for the inflow coefficient λ

$$\lambda = -\frac{\theta}{3} + \frac{1}{a}\sqrt{\left(\frac{a\theta}{3}\right)^2 + a\frac{C_{D0}}{2}}. \tag{4}$$

Introducing λ into (1), together with the solidity ratio ($c_{0.7}$: blade chord at $0.7R$)

$$\sigma_{0.7} = \frac{c_{0.7} b}{\pi R} \tag{5}$$

the rotor speed Ω of the autogyro with thrust is equal to weight $T = W$ follows from

$$\Omega = \frac{1}{R}\sqrt{\frac{W}{\frac{\sigma_{0.7} a}{2}\left(\frac{\theta}{3} + \frac{\lambda}{2}\right)\pi R^2 \rho}}. \tag{6}$$

At least, the important vertical sink speed v_{vert} of the autogyro can be determined by

$$v_{vert} = \sqrt{\frac{W}{2\pi R^2 \rho \frac{C_T}{4\lambda^2\left(\frac{C_T}{2\lambda^2} + 1\right)}}}, \tag{7}$$

C_T denotes a thrust coefficient

$$C_T = \frac{\sigma_{0.7} a}{2}\left(\frac{\theta}{3} + \frac{\lambda}{2}\right). \tag{8}$$

Table 1 shows basic data as well as the calculated rotor speed and vertical sink speed of the VPM-M16 autogyro.

Table 1: Data of the VPM-M16 autogyro

MTOW	450	kg
engine power	120	HP
maximum speed	78	kts
minimum speed	22	kts
radius of rotor	4115	mm
weight of one blade	18.2	kg
number of blades	2	
precone angle β	2.0°	
pitch angle θ	2.5°	
lift curve slope a	5.73	
profile drag coeff. C_{D0}	0.012	
blade chord $c_{0.7}$	250	mm
flapping stiffness position 1	$15.25 \cdot 10^9$	N/mm^2
flapping stiffness position 2	$2.867 \cdot 10^9$	N/mm^2
inflow coefficient λ	0.0209	
solidity ratio σ	0.0339	
rotor speed Ω	388	1/min
vertical sink speed v_{vert}	9.6	m/s

2.2 Theory of blade loading

In steady autorotation, the blade loading is independent of the angular position of the rotorblade. There is no change of rotor loading with time. Figure 1 shows the principal out-of-plane loading of a rotor blade. For this investigation, in-plane drag is not considered.

The aerodynamic lift results from local airspeed $v(r)$ and the local lift coefficient C_L (ρ air density, A reference area):

$$f_z(r) = \frac{\rho}{2} v^2(r) C_L A. \tag{9}$$

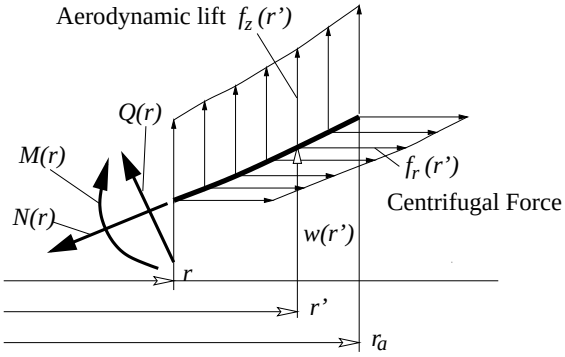

Figure 1: Loading of rotor blade

The centrifugal force $f_z(r)$ can be obtained by

$$f_r(r) = m'r\Omega^2, \tag{10}$$

where m' describes the local mass. The local airspeed $v(r)$ follows from

$$v(r) = \Omega r, \tag{11}$$

With consideration of Figure 1 the bending moment $M(r)$ is given by

$$M(r) = \int_r^{r_a} \left\{ f_z(r')(r'-r) - f_r(r')[w(r') - w(r)] \right\} dr'.$$

The bending moment $M(r)$ and the blade deformation $w(r)$ are dependent on each other. As the centrifugal forces are usually very high, therefore small deformations will have a large influence on the bending moment. Hence, this influence must not be neglected and geometrical nonlinear theory has to be used.

2.2 Rotor blades flapping moments

There are different methods to solve this problem. Hollmann proposes in [7] the matrix method, described in [8]. In [6] this procedure is used. Besides this, every other computer code for analysing geometrical nonlinear structures can be used. The following results are obtained by the use of an iterative finite element method. Data of table 1 is the basis for the following results.

Firstly, the static deflection due to blade weight of the non-rotating blade is considered (Fig. 2). In this essential load case, the bending moment acts in the opposite direction compared to flight. For fatigue life besides other load cases the number of transitions from the non-rotating rotor to the rotating rotor and vice versa (the so called start-stop cycles) are important.

Static deflection is a geometrical linear load case (no centrifugal forces). Additional load factors have to be applied when the gyroplane is taxiing over a rough taxiway, e.g. grass. Common load factors are up to 2.5.

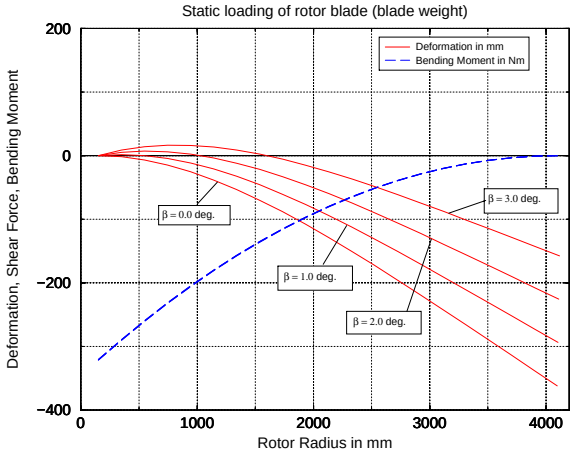

Figure 2: Flapping moment and deformation of the non-rotating blade

While deformation of the non-turning rotor blade depends on the precone angle β, the bending moment does not. The bending moment changes when the rotor is turning due to centrifugal and aerodynamic forces. Fig. 3 shows the bending moment and the deflection of the rotor blade for four different precone angles β. Precone angle is the built-in angle between the rotor blade axis and the area of rotation of the whole rotor.

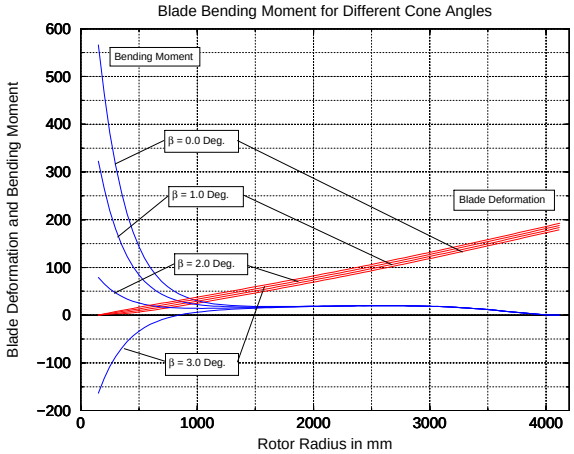

Figure 3: Flapping moment and deformation of the rotating blade and different precone angles

While all four deflection curves look very similar, the curves representing the bending moments are quite different. The largest moment results from a cone angle of $\beta = 0°$. Between $\beta = 2.0°$ and $\beta = 3.0°$ the sign of the bending moment changes.

The aerodynamic load bends the rotor blade in the upwards direction (flapping), while the centrifugal forces tend to diminish this deformation. As the bending stiffness of the rotor blade in flapping is rather small, the blade is deformed like a string in this direction, resulting from aerodynamic and centrifugal forces. Therefore, the blade deflection and the bending moment in the outer part of the rotor blade is

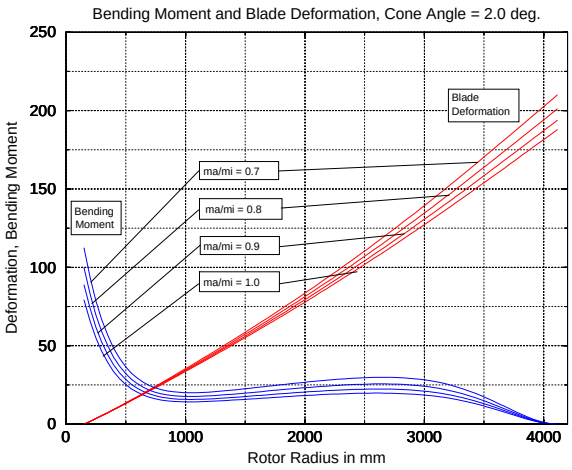

Figure 4: Flapping moment and deformation of the rotating blade for different mass distribution

nearly independent of the cone angle. Only at the cantilevered end of the blade can a difference in the loading be noticed. For a precone angle $\beta = 0°$ a relatively large bending moment occurs in comparison to the bending moment for a precone angle of $\beta = 2.0°$.

From this it follows that, for a stationary 1g flight, the ideal cone angle lies between 2.0° and 3.0°. A cone angle $\beta = 2.0°$ was chosen for the considered rotor of the M16 Gyroplane.

Another important parameter for the bending moment is mass distribution along the rotor axis. More mass in the inner part of the rotor blade decreases the centrifugal force and increases the maximum bending moment (Fig. 4).

In forward flight, the bending moments are no longer independent from the position of the blade with respect to flight direction. At the advancing blade aerodynamic lift increases while lift at the retreating blade decreases. To isolate the rotor shaft from the resulting moment, flapping hinges are necessary. The VPM-M16 autogyro has one hinge in the centre of the rotor (a so-called teetering rotor). The theory for calculating these moments is more complicated and is not shown here.

3. Experimental determination of the blade loading

To compare the theoretical determined blade loading with the real loading, the moments acting in a rotor blade during a real flight should be measured. Loading of rotor blades can be measured by strain gauges. During calibration tests relations between measured strain data and the bending moment are determined. With this data, actual blade moments can be calculated from in-flight measured strain data.

3.1 Strain measurement system

Four strains should be measured simultaneously at a data rate of at least 200 Hz. The problem in a real flight test is to transfer the measured data from the rotating rotor blade to the the fixed airframe. Professional telemetric systems as well as slip-ring systems are ruled out from the beginning due to cost reasons.

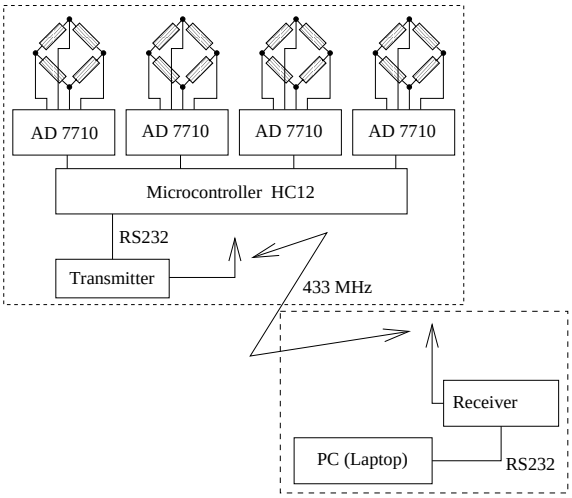

Figure 5: Principle of telemetric system

To solve the task, a small four channel telemetric system was developed (Fig. 5). It consists of four highly integrated data acquisition systems AD7710 (Analog Devices [9]), each containing an amplifier for the strain gauge signal and a 16 bit D/A-converter. These four data acquisition systems are controlled by a microcontroller 68HC12 (Motorola [10]). It controls the data acquisition and the transfer of the data to a PC, located in the airframe. This data transfer is accomplished by a wireless data link. On the rotor side a small 433 MHz transceiver module (BiM-433, Radiometrix [11]) is connected directly to the microcontroller by a conventional RS232 serial port at 38400 baud. On the receiver side, a second transceiver module receives the data and sends it to a standard PC RS232 serial port. In the PC, a small computer program receives the data bytes and saves them directly to a hard disk for analysis later. The transceiver modules allow a half duplex communication between the PC and the telemtric system.

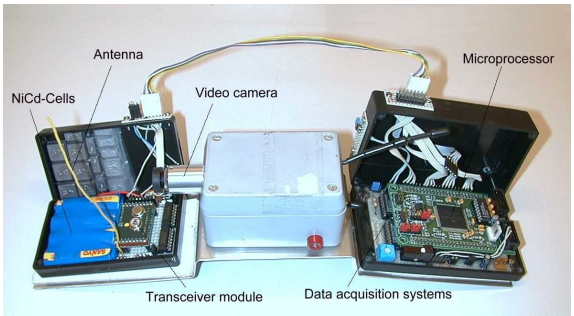

Figure 6: Telemetric system

Fig. 6 and 7 show a first prototype of the described strain measurement system. In addition to this, a small video camera with a 2.4 GHz video signal transmitter can be seen. The video signal is recorded by a

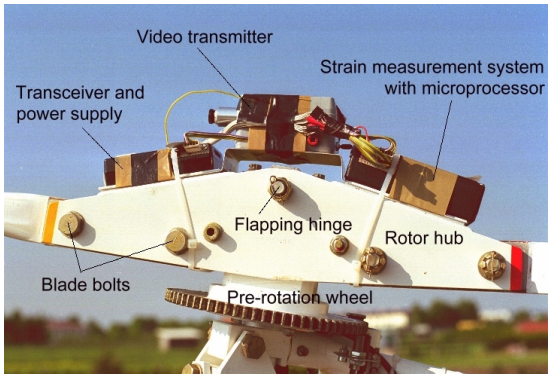

Figure 7: Strain measurement and telemetric system

video recorder, also located in the airframe. By means of this camera, the motion of one blade can be observed. This supplements the analysis of the strain gauge data.

Due to the very simple protocol (serial at 38400 baud) and the wireless data transfer between the rotating and the fixed system some loss of data cannot be avoided. The relatively high data rate (more than 200 Hz) allows for some data bytes to be missing from the sequence. However, it is essential to know whether there are bytes missing or not. To accomplish this besides the strain data some additional bytes are transmitted, synchronisation bytes and one count byte. Figure 8 shows the used protocol for one data frame.

4 sychronisation bytes:

0AAh	001h	0FFh	0FBh

up to 11 data bytes:

Channel	Counter		
Ch0 high	Ch0 low	Ch1 high	Ch1 low
Ch2 high	Ch2 low	Ch3 high	Ch3 low
supply voltage			

Figure 8: Transmitted bytes for one data frame

The first three bytes are for synchronisation purposes of the RS232 UART at the receiver side, the fourth byte, 0FBh, defines the beginning of each data frame. When this byte is received, up to eleven data bytes following it are recorded. The first data byte is a binary representation of the channels to be measured. To achieve a higher rate of measurements per second it is possible to transfer the data of less than four channels. The counter byte simply counts from 0 to 255. By observing this byte, up to 254 missing data frames can be detected. In a later analysis, missing data may be inserted by interpolating between known data. Each strain value is transmitted as a signed 16 bit binary integer word. The strain gauge data is followed by the voltage of the supplying NiCd-battery.

A maximum of 15 bytes are to be transferred for each data frame. At a baud rate of 38400 with one start and one stop bit, 3840 bytes/second can be transmitted. So, 256 data frames can be recorded per second. This is more than originally required. When measuring only one channel without supply voltage, a data frame consits of eight bytes, which leads to 480 measurments per second.

Figure 9 shows the uncorrected measured strain data. A lot of failures are visible. However, compared to the whole number of data frames (200/s) the absolute number of errors is small (less than 1%). Many of these errors can be detected and eliminated.

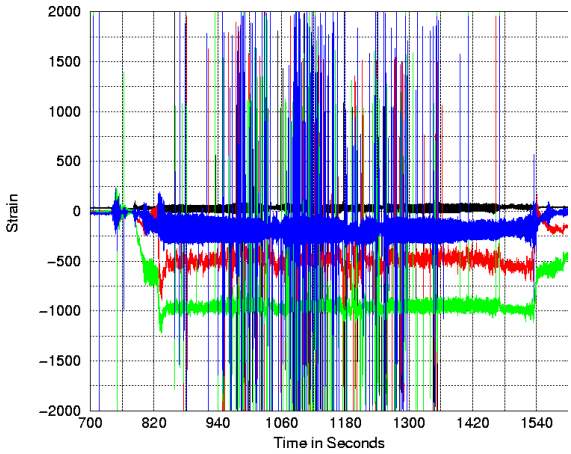

Figure 9: Uncorrected strain data

Besides missing data frames other types of errors are possible. For example, single wrong data bytes are more difficult to find. Most of them can be detected by comparing successive strain data (low pass filtering). Data which does not fit to neighbouring values are deleted and substituted again by interpolated data. In this way, most data errors can be detected and corrected. The accuracy of this procedure seems to be sufficient for this application. In Fig. 10 and 13 some spikes can still be seen. If necessary, these spikes can be deleted by hand. In the present work, this is not done, the spikes are purely neglected in the interpretation of the data. Figure 10 shows the same data as Fig. 9, but after error analysis. Nearly all errors could be deleted.

3.2 Instrumented blade

Three types of blade loading are to be determined:

1. flapping moments at three radial positions,
2. one lead-lag moment and
3. one torsional moment.

The lead-lag and the torsional moment should be measured at the same radial position as one of the flapping moments. According to Figure 3 the flapping moment decreases rapidly from the cantilevered end in radial direction. Therefore the strain gauge bridges for the flapping moment are located near this end. A distance of 500 mm between the measurement stations is chosen. Lead-lag and torsional moments are

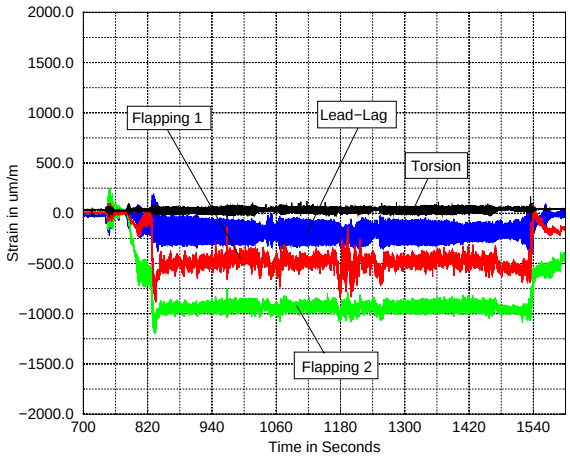

Figure 10: Corrected strain data

measured at the second flapping measurement point. The radial positions of the strain gauge bridges are shown in Fig. 11.

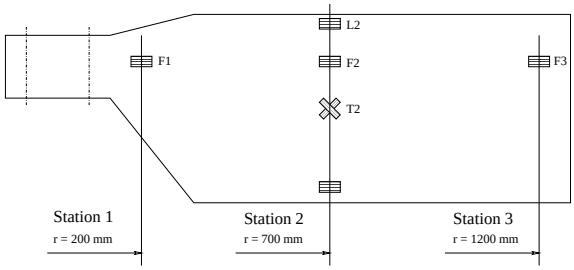

Figure 11: Location of the strain gauges bridges on the rotor blade

The strain gauges of different Wheatstone bridges are located in such a manner that the different types of loading hardly influence each other. This is excellent for the flapping moment and the torsional moment. However, due to geometrical reasons the lead-lag bridge shows some strain due to flapping. This influence is considered in the later analysis.

3.3 Test flight

The measurement system is mounted on the rotor hub as shown in Fig. 7. A laptop for storing the strain data and a video recorder are located inside the airframe. In the first flight, four strain data are measured: flapping at stations 1 and 2 as well as lead-lag bending and torsion. The third flapping moment is to be measured later. Fig. 12 shows a VPM M16 Autogyro during takeoff. Such a type is used for the flight tests.

Fig. 13 shows the strain data of the first test flight. Different phases of the flight can be clearly distinguished. At the beginning of the test, all strain gauge bridges are put to zero. Then the autogyro rolled with a non-turning rotor over a grass taxiway to the runway. After a short stop, take off follows. Some manoeuvres, including a nearly steady autorotation follow after about three minutes. Then the autogyro returned to the airfield. With touch down and taxiing the first test flight ends.

Figure 12: A VPM M16 autogyro during take off

By using the calibration test data, moments can be calculated from strain data. In doing so, it must be considered that the strain gauge bridges are set to zero at the beginning of the test flight. In this condition, the blades are loaded in flapping by their own weight. Fig. 2 shows that these flapping moments can not be neglected, they must be added to the measured flapping moment. In Fig. 13 the resulting flapping, lead-lag and torsional moments are shown.

One can see that the largest absolute flapping moments occur when the autogyro is taxiing over a rough runway. After take off, these flapping moments become nearly zero for normal 1g flight conditions. At the time coordinate 620 sec. in Fig. 14 the flight condition “steady autorotation” is reached, of course not exactly, but approximately. We see very low amplitudes for all moments (see Fig. 14), torsional and flapping moment 1 nearly zero, the mean value of lead-lag and flapping moment 2 comes to about 50 Nm and -50 Nm respectively. When manoeuvring, only the flapping moment at the joint connecting the blade to the rotor hub increases. The flapping moment at radius station 2 ($r = 700$ mm) hardly changes (Fig. 14 left side). The reason for this is the flexibility of the rotor blade in flapping direction. In the transition from one flight condition to another, additional moments occur. Also the amplitude of the lead-lag moment increases. Additional, higher harmonic frequencies are included (e.g. Fig. 14 right side, transition from forward flight to pure autorotation).

In general, the first test flight has shown the utility of the developed strain measurement and telemetric system from which reliable data could be acquired. Data analysis yields blade moments, which can be interpreted by the causing flight condition. To get an exact correlation between blade load and flight condition, additional data such as flight speed, rate of climb, rotational speed of rotor and propeller, etc. has to be recorded.

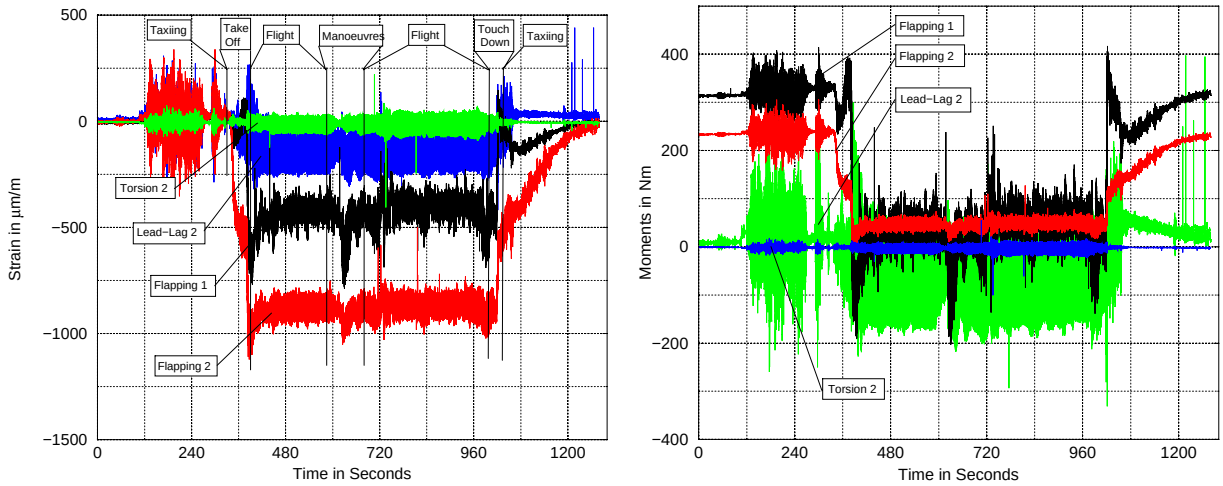

Figure 13: Strains measured during first test flight

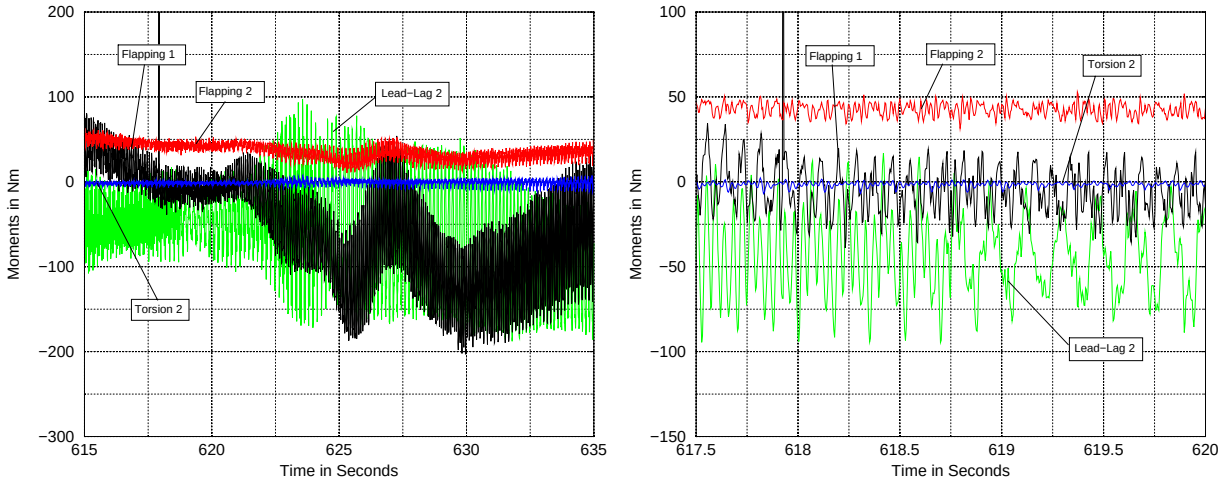

Figure 14: Moments during some manoeuvres

3.4 Video transmission

As shown in Fig. 6 and 7 a small video camera is mounted on the rotor hub. A conventional video transmitter in the 2.4 GHz band is used to transmit the video signal to a receiver, connected to a camcorder with line input. The camera looks at the instrumented rotor blade. Blade deformation can be observed and the airflow over the profile can be determined by wool strings. Figure 15 shows some pictures from a video sequence. The change of airflow along one revolution, especially the backflow at the retreating blade, is clearly visible.

The standard for the CCIR video is 25 pictures per second. At a nominal rotational speed of 388 revolutions per minute, 6.5 pictures per revolution can be acquired. This rather low picture rate can be increased by combining pictures of successive rotations in a correct sequence. If the flight condition does not change, this method of rearranging single pictures yields very good results. The new sequence looks like a real slow motion film. Up to 30 pictures per revolution (about 200 pitcures per second) could be achieved.

4. CONCLUSIONS

Blade loads of a VPM M16 autogyro were determined theoretically and experimentally. For the theoretical investigation, only the simple load case “steady autorotation” was considered. Due to the high centrifugal forces geometrical non-linear theory must be used.

Results show that the largest flapping moments occur when the rotor is not rotating, e.g. when taxiing over a grass taxiway. The precone angle of the rotor blades is chosen in such a manner that under normal flight conditions the flapping moments are minimal. Flight tests verify the correct precone angle.

To accomplish flight tests, the problem of transmitting the strain gauge data from the rotating system rotor to the fixed system airframe was to be solved. A simple wireless four-channel telemetric system was developed and tested successfully. With some special software for data storing and error detection a data rate of 250 Hz for four channels, 16 bits each, could be achieved.

Flight tests with this system show the practicability

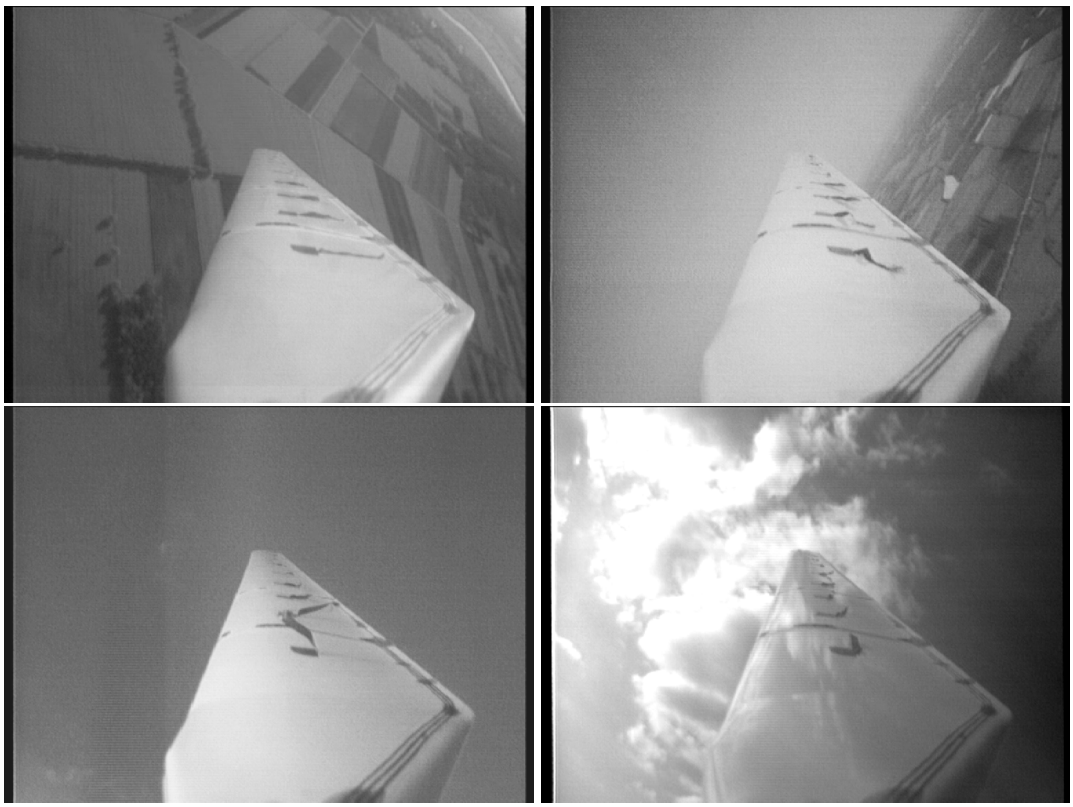

Figure 15: Video sequence of the rotorblade in flight

of such a measurement system. For the near future, the system is to be extended for additional measuring some flight data such as speed, altitude, positions of controls and others.

A transmission of videosignals to optically observe the blade motion and the airflow is in test, too. It was possible to increase the picture rate above the common video norm by rearranging the pictures of successive rotations. In this way, up to 300 pictures per second could be achieved.

Next, all acquired data is to be analysed in detail. The aim is to verify the flying characteristics as well as the strength of the rotor blades and the other structures.

ACKNOWLEDGEMENT: This work is supported by Hochschule Bremen, University of Applied Sciences of Freie Hansestadt Bremen, Germany and by ARROW Engines (UK), Ltd.

REFERENCES

1. De la Cierva, Rose D.; *Wings of Tomorrow*, Brewer, Warren & Putnam, New York, 1931
2. Nikolsky A.A.; *Helicopter Design Theory*, Princeton University Press, Princeton, 1945
3. Payne P.R.; *Helicopter Dynamics and Aerodynamics*, Pitman & Sons, London, 1959
4. McKillip R.M., Chih M.H.; *Instrumented Blade Experiments Using a Light Autogyro*, 16th European Rotorcraft Forum, Glasgow, Scotland, September 18-20, 1990
5. Houston S.S. *Identification of gyroplane lateral/directional stability and control characteristics from flight test*, Proc. of the Inst. of Mech. Eng. Part G, Journal of Aerospace Engineering, 212(G4), 271-285, 1998
6. Noll S.; *Untersuchung der Beanspruchung eines Tragschrauberrotors*, Diplomarbeit, Hochschule Bremen, Mechanical Engineering, Bremen, 1999
7. Hollmann M.; *Modern Gyroplane Design*, Aircraft Designs Inc., Monterey, CA, 1992
8. Mayo A.P.; *Matrix Method for Obtaining Spanwise Moments and Deflections of Torsionally Rigid Rotor Blades with Arbitrary Loadings*; NACA TN 4304, 1958
9. N.N.; *AD7710, LC^{2}MOS Signal Conditioning ADC*; Analog Devices, USA, 1995
10. N.N.; *MC68HC812A4 16-Bit Microcontroller*, Technical Data, Motorola, USA, 1997
11. N.N.; *BiM-433, Low Power UHF Data Transceiver Module*, Data Sheet, Radiometrix, Hertfordshire, England, 1998